SANG-IN LEE[1], SEUNG-HYEOK SHIN[1], HYEONWOO PARK[2],
HANSOO KIM[2], JOONHO LEE[2*], BYOUNGCHUL HWANG[1*]

# IN-SITU OBSERVATION OF ACICULAR FERRITE TRANSFORMATION IN HIGH-STRENGTH LOW-ALLOY STEEL USING CONFOCAL LASER SCANNING MICROSCOPY

In-situ observation of the transformation behavior of acicular ferrite in high-strength low-alloy steel using confocal laser scanning microscopy was discussed in terms of nucleation and growth. It is found that acicular ferrite nucleated at dislocations and slip bands in deformed austenite grains introduced by hot deformation in the non-recrystallization austenite region, and then proceeded to grow into an austenite grain boundary. According to an ex-situ EBSD analysis, acicular ferrite had an irregular shape morphology, finer grains with sub-grain boundaries, and higher strain values than those of polygonal ferrite. The fraction of acicular ferrite was affected by the deformation condition and increased with increasing the amount of hot deformation in the non-recrystallization austenite region.

*Keywords:* acicular ferrite; high-strength low-alloy steel; confocal laser scanning microscopy (CLSM); phase transformation, in-situ observation

## 1. Introduction

Acicular ferrite has been reported as a microstructure with the potential to achieve both high strength and good toughness because the plates of acicular ferrite nucleate intragranularly on non-metallic inclusions within large austenite grains in weld steels, and then grow in many different orientations maintaining an orientation relationship with the austenite [1-11]. In the high-strength low-alloy (HSLA) steels, however, acicular ferrite is defined as a highly sub-structured and non-equiaxed ferrite that forms on continuous cooling [12-19]. Despite the morphological similarity, the condition for forming acicular ferrite in HSLA steels differs significantly from that in weld steels because non-metallic inclusions for nucleation sites are limited in HSLA steels. Therefore, researchers confuse the naming of acicular ferrite because there are differences in the classification methods of acicular ferrite between weld steels and HSLA steels. For these reasons, the morphological characteristics and transformation behavior of acicular ferrite are still controversial and remain unresolved, so it is necessary to elucidate the mechanism of acicular ferrite transformation in HSLA steels.

Meanwhile, confocal laser scanning microscopy (CLSM) is regarded as an effective approach to analyze dynamic phase transformation behavior, and this method can be used directly to observe the nucleation and growth of phases in steels during the heating, isothermal transformation, and continuous cooling processes [20-24]. Wu et al. [20] investigated the three-dimensional morphology and growth behavior of intergranular acicular ferrite using CLSM and electron backscattered diffraction analysis. According to their results, intergranular acicular ferrite had a plate-like morphology with numerous pits and defects as well as sub-grains. Tian et al. [21] reported that bainitic transformation was directly observed by CLSM during an austempering treatment above the martensite start temperature.

Although studies on the CLSM analysis reported so far only considered phase transformation behavior according to the heat treatment conditions, in-situ observations of acicular ferrite transformation in HSLA steels according to the hot deformation in the non-recrystallization austenite region have rarely been carried out using CLSM. In this study, therefore, the influence of the hot deformation condition on the transformation behavior of acicular ferrite was investigated using CLSM and the mechanism of acicular ferrite transformation in HSLA steels was confirmed through in- and ex-situ observations by means of CLSM and electron backscatter diffraction (EBSD) analyses, respectively.

[1] SEOUL NATIONAL UNIVERSITY OF SCIENCE AND TECHNOLOGY, DEPARTMENT OF MATERIALS SCIENCE AND ENGINEERING, SEOUL, 01811, REPUBLIC OF KOREA
[2] KOREA UNIVERSITY, DEPARTMENT OF MATERIALS SCIENCE AND ENGINEERING, SEOUL, 02841, REPUBLIC OF KOREA

* Corresponding authors: bhwang@seoultech.ac.kr, joonholee@korea.ac.kr

## 2. Experimental

The HSLA steel used in this study had a chemical composition of Fe-0.06C-0.25Si-1.55Mn-0.25(Ni+Cr+Mo)-0.04Nb (wt.%). Based on the chemical composition of the steel, the non-recrystallization temperature ($T_{nr}$), the $A_3$ temperature, the bainite start temperature ($B_s$), and the martensite start temperature ($M_s$) were calculated to determine the in-situ observation condition of acicular ferrite transformation using a CLSM system [25]. The $T_{nr}$, $A_3$, $B_s$, and $M_s$ of the steel investigated in this study were 974°C, 850°C, 615°C, and 450°C, respectively. The effect of the hot deformation condition on the transformation behavior of acicular ferrite was investigated by using a CLSM system (VL2000DX-SVF17SP/15FTC, Yonekura, Japan) equipped with a deformation station [26-28]. Sheet-type tensile specimens with a gauge diameter of 5.0 mm and a gauge length of 12.5 mm were used for the CLSM analysis. As shown in the schematic diagram of the thermal treatments and deformation conditions for the in-situ observation with the CLSM system (Fig. 1), the specimen was heated to 1,000°C at a rate of 15°C/s, isothermally held for 60 s for sufficient formation of the austenite grain, and then cooled to 900°C at a rate of 2°C/s for hot deformation in the non-recrystallization austenite region. Hot deformation of 30% and 50% at 900°C was applied to the specimen at a crosshead speed of 20 mm/min. After hot deformation, the specimen was cooled to 700°C at a rate of 3°C/s for phase transformation and then held for 15 min. Finally, the specimen was cooled to room temperature at a rate of 10°C/s. The microstructure features of the specimen processed by CLSM were observed by an EBSD (e-FlashHR, Bruker Nano, Germany) analysis. The EBSD specimens were mechanically polished and then electro-polished in a mixed solution of 60% methanol ($CH_3OH$), 35% butoxyethanol ($C_6H_{14}O_2$), and 5% perchloric acid ($HClO_4$). The EBSD results were processed using orientation imaging microscopy (OIM) analysis software (TexSEM Laboratories, Inc., UT, USA).
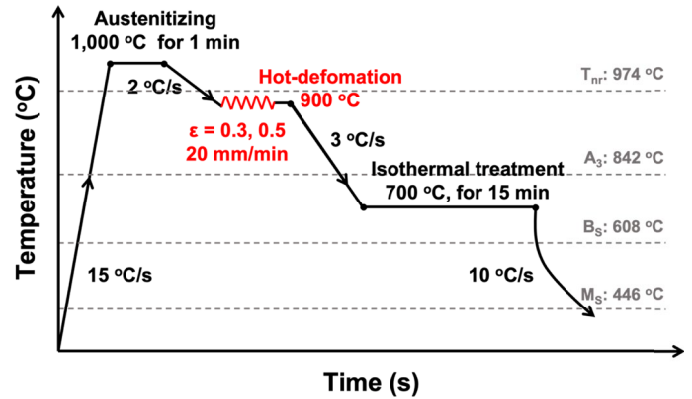


Fig. 1. Schematic diagram of the thermal treatments and deformation conditions for the in-situ observation under the CLSM system. $T_{nr}$, $A_3$, $B_s$, and $M_s$ are the non-recrystallization temperature, the $A_3$ temperature, the bainite start temperature, and the martensite start temperature, respectively

## 3. Results and discussion

Fig. 2 exhibits the CLSM images at the stages of initial, austenitizing, 0% deformation, 10% deformation, 30% deformation,
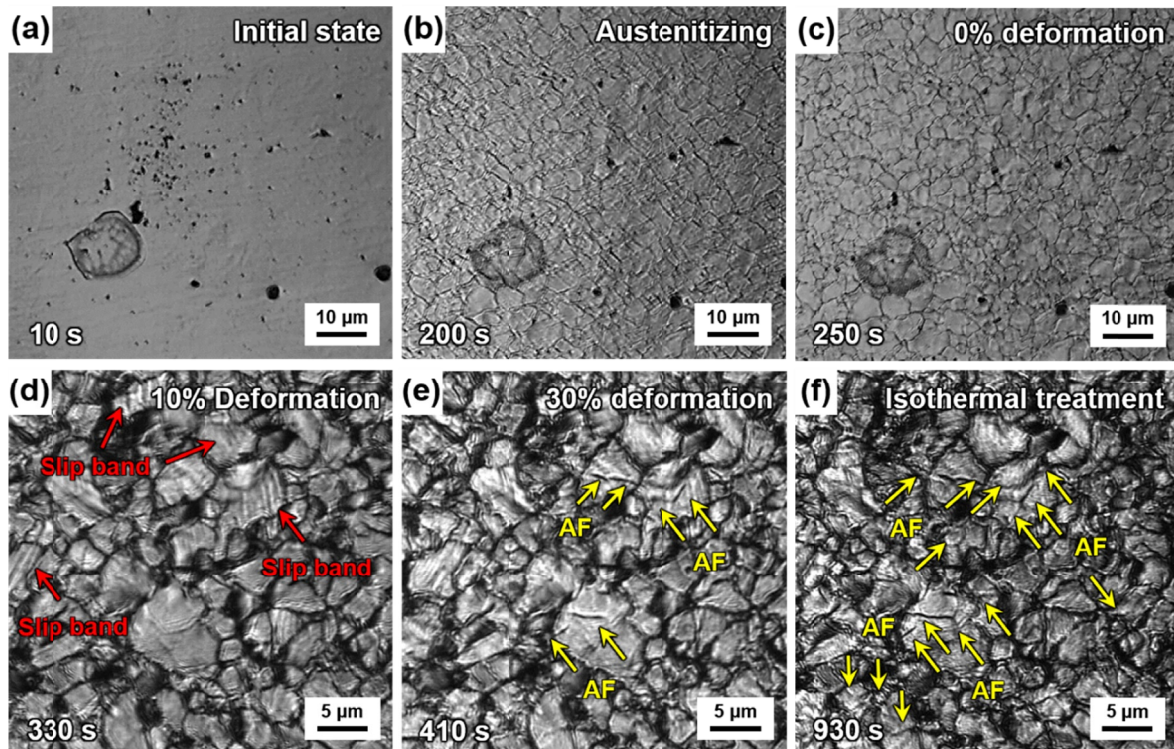


Fig. 2. CLSM images at the stages of (a) initial, (b) austenitizing, (c) 0% deformation, (d) 10% deformation, (e) 30% deformation, and (f) isothermal treatment which correspond to 10 s, 200 s, 250 s, 330 s, 410 s, and 930 s, respectively, of the specimen hot deformed at 30% strain. The red and yellow arrows indicate slip bands and acicular ferrite (AF) grains, respectively

and isothermal treatment of the specimen hot deformed at 30% strain. Before the temperature increase, grains were not seen in the initial stage (Fig. 2(a)), whereas austenite with a grain size of about 10 μm appeared after austenitizing was conducted at 1,000°C for 60 s (Fig. 2(b)). Comparing the CLSM images before and after deformation (Figs. 2(c) and (d)), it can be seen that the prior austenite grains were elongated with tensile deformation and slip bands (red arrows) formed generally in the austenite grains. As shown in Figs. 2(e) and (f), the acicular ferrite grains nucleate at the slip bands generated inside the deformed austenite grains immediately after the isothermal treatment after 30% strain and then grow in an irregular direction to the prior austenite grain boundary or adjacent acicular ferrite grains. From

these in-situ CLSM observations, it was mainly confirmed that acicular ferrite in HSLA steels nucleates at slip bands or dislocations in deformed austenite grains by means of hot deformation in the non-recrystallization austenite region, unlike weld steels.

The transformation behavior of acicular ferrite in HSLA steel has been studied through in-situ CLSM observations. More detailed ex-situ crystallographic features of the acicular ferrite were conducted by an EBSD analysis which is a very useful technique to examine the orientation features of selected grains. In the present study, the misorientation characteristics between microstructures formed by the CLSM process were investigated through the EBSD technique. Figs. 3(a) and (b) show the EBSD inverse pole figure (IPF) map, misorientation angles, and ker-
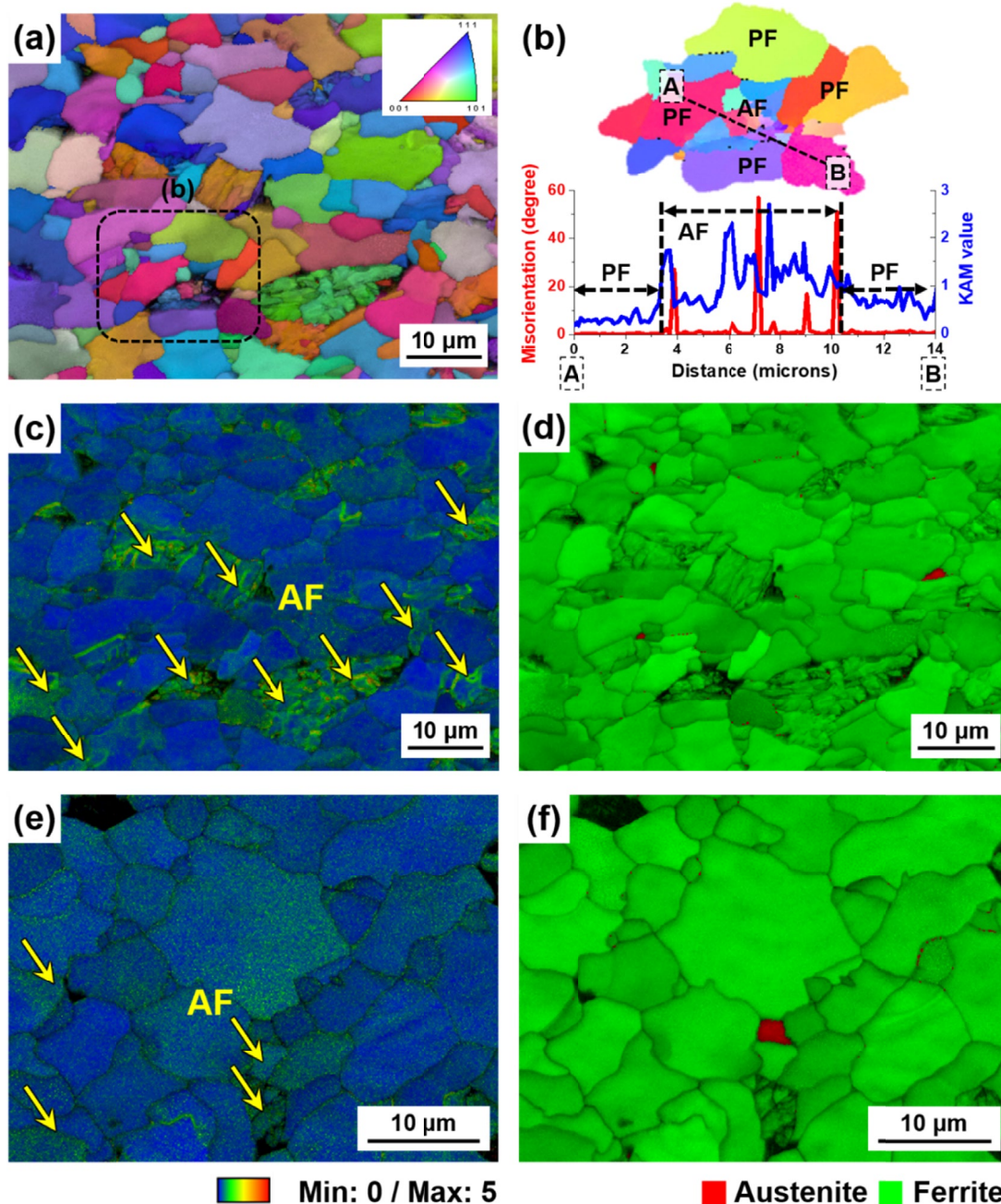


Fig. 3. EBSD inverse pole figure (IPF), kernel average misorientation (KAM), and phase maps of the specimens hot deformed at (a)-(d) 50% and (e)-(f) 30% strains: (a) IPF map, (b) misorientation angles and KAM values of acicular ferrite, (c) and (e) KAM maps, and (d) and (f) phase maps. The acicular ferrite (AF) grains were indicated by the yellow arrows in the KAM maps

nel average misorientation (KAM) values of the specimen hot deformed at 50% strain. The acicular ferrite has finer grains with sub-grain boundaries and higher KAM values compared to the PF. According to the previous studies [25,29,30], HSLA steels fabricated by the recently developed thermomechanical controlled process (TMCP) have very complex microstructures consisting of polygonal ferrite, acicular ferrite, granular bainite, bainitic ferrite, and martensite-austenite constituent. Especially, it is known that acicular ferrite has an irregular shape morphology, fine grains aligned in an arbitrary direction, and sub-grain boundaries [29]. As a result, it is mainly identified that microstructural features such as the morphological, misorientation, and KAM characteristics observed by an EBSD analysis can be a guideline for classifying acicular ferrite among the complex microstructures fabricated by TMCP.

Figs. 3(c) to (f) indicate the EBSD KAM and phase maps of the specimens hot deformed at 30% and 50% strains. Acicular ferrite grains were indicated by the yellow arrows in the KAM maps. Based on the microstructural features of the acicular ferrite observed by the EBSD analysis (Fig. 3(b)), it is clearly observed that the fraction of the acicular ferrite increased with increasing the strain at a high temperature. Generally, it is reported that acicular ferrite in HSLA steels fabricated by TMCP has fine and irregular shaped grains because it nucleates at deformed bands within the austenite grain introduced by a severe rolling reduction in the non-recrystallization region [31]. In HSLA steels, the fraction of acicular ferrite is generally affected by the chemical composition and thermo-mechanical control process conditions [12-14]. Zhao and Palmiere [12] reported that the fraction of the

acicular ferrite was increased with decreasing prior austenite grain size in HSLA steels. Also, Kim et al. [13] evaluated the transformation behavior and microstructural characteristics of acicular ferrite in linepipe steels. These results indicated that the fraction of acicular ferrite increased when the strain during hot deformation in the non-recrystallization austenite region was increased because acicular ferrite nucleates mostly at deformed austenite bands caused by hot deformation in the non-recrystallization austenite region. Accordingly, it is reasonable that the fraction of acicular ferrite increased with increasing the strain at hot temperature because the nucleation sites of dislocations and slip bands within the austenite grains increased according to the increment of the strain during hot deformation in the non-recrystallization austenite region.

Quantitative characterization through in-situ CLSM observation and ex-situ EBSD analysis enables a clearer understanding of the transformation behavior of acicular ferrite in HSLA steels. Based on the results above, schematic illustrations showing the transformation behavior of acicular ferrite in weld steels and HSLA steels are presented in Fig. 4. It can be clearly seen that the phase transformation of acicular ferrite in terms of nucleation and growth is different in weld steels and HSLA steels. In the case of the weld steels (Fig. 4(a)), acicular ferrite nucleates at metallic inclusions within the austenite grains and then grows in needle-like morphology [2-4]. On the other hand, the prior austenite grain is elongated in the tensile direction by hot deformation in the non-recrystallization austenite region, resulting in the formation of dislocations and slip bands within the austenite grains, which act as nucleation sites for the transformation of
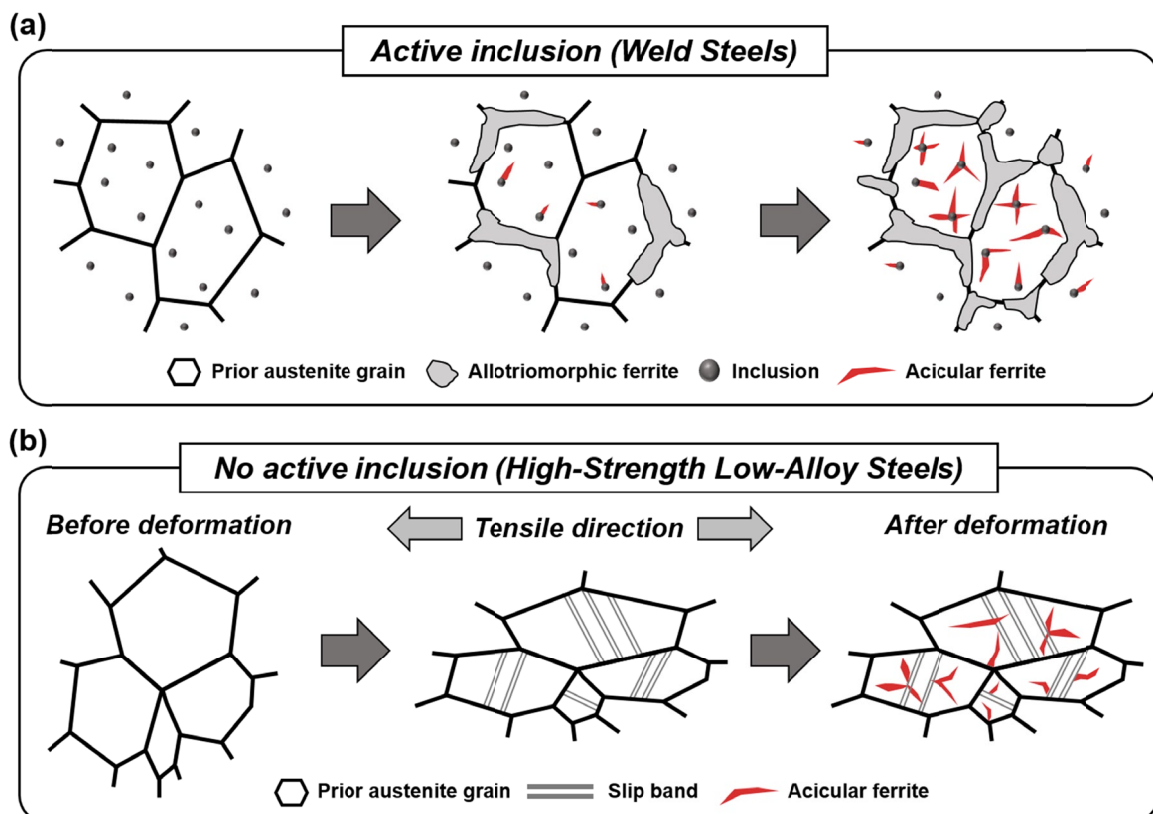


Fig. 4. Schematic illustrations showing the transformation behavior of acicular ferrite in the (a) weld steels and (b) high-strength low-alloy steels

acicular ferrite. Therefore, acicular ferrite in HSLA steels nucleates at dislocations and slip bands within the austenite grains during isothermal or cooling treatments (Fig. 4(b)).

## 4. Conclusions

To conclude, in-situ observation and the mechanism of acicular ferrite transformation according to the hot deformation conditions in the non-recrystallization austenite region could be understood by a CLSM analysis. It is successfully confirmed that acicular ferrite was nucleated at dislocations and slip bands in deformed austenite grains introduced by hot deformation in the non-recrystallization austenite region, and then proceeded to grow into an austenite grain boundary. An ex-situ EBSD analysis revealed that the acicular ferrite had an irregular shape morphology, finer grains with sub-grain boundaries, and higher KAM values compared to those of the PF, and their fraction was increased with an increasing amount of hot deformation in the non-recrystallization austenite region.

## REFERENCES

[1] Y.E. Smith, A.P. Coldren, R.L. Cryderman, Climax Molybdenum Company Ltd., Toward Improved Ductility and Toughness, pp. 119-142,Tokyo 1972.

[2] C.H. Lee, H.K.D.H. Bhadeshia, H.C. Lee, Mater. Sci. Eng. A **360**, 249 (2003).

[3] A.F. Gourgues, H.M. Flower, T.C. Lindley, Mater. Sci. Technol. **16**, 26 (2000).

[4] H.K.D.H. Bhadeshia, The Institute of Materials, Bainite in Steels (Transformations, Microstructure, and Properties), London 2001.

[5] N. Amirijani, M. Ketabchi, M. Eskandari, M. Hizombor, Met. Mater. Int. **27**, 4802 (2021).

[6] Y.J. Oh, S.Y. Lee, J.S. Byun, Mater. Trans. JIM **41**, 1663 (2000).

[7] M. Díaz-Fuentes, A. Iza-Mendia, I. Gutiérrez, Metall. Mater. Trans. A, **34**, 2505 (2003).

[8] L.R. Jacobo, R. García-Hernández, V.H. López-Morelos, A. Contreras, Met. Mater. Int. **27**, 3750 (2021).

[9] S.I. Lee, S.Y. Lee, J. Han, B. Hwang, Mater. Sci. Eng. A **742**, 334 (2019).

[10] S.Y. Lee, S.I. Lee, B. Hwang, Mater. Sci. Eng. A, **711**, 22 (2018).

[11] K. Seo, K.H. Kim, H.J. Kim, H. Ryoo, G.M. Evans, C. Lee, Met. Mater. Int. **26**, 1226 (2020).

[12] H. Zhao, E.J. Palmiere, Mater. Charact. **145**, 497 (2018).

[13] Y.M. Kim, H. Lee, N.J. Kim, Mater. Sci. Eng. A **478**, 361 (2008).

[14] F. Xiao, B. Liao, D. Ren, Y. Shan, K. Yang, Mater. Charact. **54**, 305 (2005).

[15] T. Araki, Atlas for Bainitic Microstructures, ISIJ, Tokyo 1992, pp. 1-100.

[16] P. Korczak, H. Dyja, J.W. Pilarczyk, Met. Mater. Int. **4**, 707 (1998).

[17] M.C. Zhao, K. Yang, F.R. Xiao, Y.Y. Shan, Mater. Sci. Eng. A, **355**, 126 (2003).

[18] Y.M. Kim, S.K. Kim, Y.J. Lim, N.J. Kim, ISIJ Int. **42**, 1571 (2002).

[19] S.W. Thompson, D.J. Colvin, G. Krauss, Scr. Metall. **22**, 1069 (1988).

[20] S. Wu, C. Zhang, L. Zhu, Q. Zhang, X. Ma, Scr. Mater. **185**, 61 (2020).

[21] J. Tian, G. Xu, Z. Jiang, H. Hu, Q. Yuan, X. Wan, Met. Mater. Int. **26**, 961 (2020).

[22] I. Sohn, R. Dippenaar, Metall. Mater. Trans. B **47**, 2083 (2016).

[23] Y. Shen, B. Chen, C. Wang, Metall. Mater. Trans. A **51**, 3371 (2020).

[24] S. Clark, V. Janik, A. Rijkenberg, S. Sridhar, Mater. Charact. **115**, 83 (2016).

[25] S.I. Lee, S.Y. Lee, S.G. Lee, H.G. Jung, B. Hwang, Met. Mater. Int. **24**, 1221 (2018)

[26] C.S. Li, Z.X. Li, J.Y. Ren, X.Y. Tu, B.Z. Li, Steel Res. Int. **90**, 1800470 (2019).

[27] Q. Luo, H. Chen, W. Chen, C. Wang, W. Xu. Q. Li, Scr. Mater. **187**, 413 (2020).

[28] S.W. Ko, H.W. Park, I. Yoo, H. Kim, J. Lee, B. Hwang, Arch. Metall. Mater. **66**, 1019 (2021).

[29] S.I. Lee, J. Lee, B. Hwang, Mater. Sci. Eng. A **758**, 56 (2019).

[30] S.I. Lee, B. Hwang, J. Iron Steel Res. Int. **27**, 319 (2020).

[31] J.S. Kang, J.B. Seol, C.G. Park, Mater. Charact. **79**, 110 (2013).